Evidence for a photoinduced nonthermal superconducting-to-normal-state phase transition in overdoped $Bi_2Sr_2Ca_{0.92}Y_{0.08}Cu_2O_{8+\delta}$

G. Coslovich,[1,2] C. Giannetti,[3] F. Cilento,[1,2] S. Dal Conte,[4] G. Ferrini,[3] P. Galinetto,[4] M. Greven,[5] H. Eisaki,[6] M. Raichle,[7] R. Liang,[7,8] A. Damascelli,[7,8] and F. Parmigiani[1,9]

[1]*Department of Physics, Università degli Studi di Trieste, Trieste I-34127, Italy*
[2]*Laboratorio Nazionale TASC, AREA Science Park, Basovizza Trieste I-34012, Italy*
[3]*Department of Physics, Università Cattolica del Sacro Cuore, Brescia I-25121, Italy*
[4]*Department of Physics A. Volta, Università degli Studi di Pavia, Pavia I-27100, Italy*
[5]*School of Physics and Astronomy, University of Minnesota, Minneapolis, Minnesota 55455, USA*
[6]*Nanoelectronics Research Institute, National Institute of Advanced Industrial Science and Technology, Tsukuba, Ibaraki 305-8568, Japan*
[7]*Department of Physics & Astronomy, University of British Columbia, Vancouver, British Columbia V6T 1Z1, Canada*
[8]*Quantum Matter Institute, University of British Columbia, Vancouver, British Columbia V6T 1Z4, Canada*
[9]*Sincrotrone Trieste S.C.p.A., Basovizza I-34012, Italy*

(Received 21 May 2010; revised manuscript received 23 December 2010; published 28 February 2011)

Here we report extensive ultrafast time-resolved reflectivity experiments on overdoped $Bi_2Sr_2Ca_{1-x}Y_xCu_2O_{8+\delta}$ single crystals ($T_c = 78$ K) aimed to clarify the nature of the superconducting-to-normal-state photoinduced phase transition. The data show a lack of the quasiparticle decay time divergence at the fluence required to induce this phase transition, in contrast to the thermally driven phase transition observed at T_c and at variance with recently reported photoinduced transitions from charge-density and spin-density waves to a metal. Our data demonstrate the nonthermal character of the superconducting-to-normal-state photoinduced phase transition. The data are analyzed using an *ad-hoc* time-dependent Rothwarf-Taylor model, opening the question of the order of this nonequilibrium phase transition.

DOI: 10.1103/PhysRevB.83.064519 PACS number(s): 74.40.Gh, 78.47.jg, 74.72.−h

I. INTRODUCTION

The possibility of inducing an electronic nonthermal phase transition in high-temperature superconductors (HTSCs), by means of ultrashort laser pulses, constitutes a new path for studying the origin of the superconductivity in these materials. In fact, under such nonequilibrium conditions, the homogeneous superconducting phase becomes unstable as its free energy increases during the pulse duration,[1–3] while the superconducting order parameter can coexist with a pseudogap or the normal state. For many years the exploration of the physics of this process has been a difficult task because of experimental limitations, mainly arising from laser-induced heating of the samples.[4–7] Only recent all-optical pump-probe experiments[3,8,9] on underdoped and optimally doped HTSCs have achieved control of the impulsive vaporization of the superconducting condensate in the high-intensity regime. This phenomenon has been observed as the saturation of the transient reflectivity variation ($\Delta R/R$) signal associated with the superconducting phase,[3,8] in contrast to its linear fluence dependence in the low-intensity regime.[6,10–14]

A similar photoinduced phase transition (PIPT) to the metallic phase has been reported recently for charge-density-wave[15,16] (CDW) and spin-density wave[17] (SDW) compounds. While in such systems the PIPT exhibits quasithermal character, as it is accompanied by the same critical slowing down observed in quasi-equilibrium at T_c,[15–17] the origin of the PIPT in HTSCs remains unclear. A picture of the photoinduced nonequilibrium state is still lacking due to intrinsic difficulties in disentangling pseudogap and normal-phase signals in optimally and underdoped samples,[3,9] the fingerprint of the pseudogap phase being the $\Delta R/R$ sign change observed above T_c in pump-probe experiments when probing at 800 nm wavelength.[18]

Here we report pump-probe optical reflectivity measurements at 800 nm in the high-excitation regime on an overdoped $Bi_2Sr_2Ca_{0.92}Y_{0.08}Cu_2O_{8+\delta}$ (Y-Bi2212) single crystal ($T_c = 78$ K). In this doping regime, the underlying normal phase is Fermi-liquid-like[19] and no $\Delta R/R$ sign change above T_c is measured, at variance with optimally and underdoped samples.[20] These characteristics are fundamental to quantitatively interpret the data within a Rothwarf-Taylor (RT) model with time-dependent parameters.

We show a lack of the quasiparticle decay time increase at the fluence required to photoinduce the transition, at variance with previously reported PIPTs on CDW (Refs. 15,16) and SDW (Ref. 17) systems and in contrast to the decay time divergence observed at T_c in cuprates.[10,11,13] This finding demonstrates the nonthermal character of the superconducting-to-normal-state PIPT, raising the question of the nature of this phase transition. To address this question we develop a time-dependent RT model. The measured decay dynamics is well reproduced by this model, resulting in a nonequilibrium superconducting gap of about one-half of the equilibrium value at the pump fluence threshold for the PIPT. We propose two different pictures of the nonthermal phase transition observed in the experiment.

The present work represents a landmark for the growing field of pump-probe techniques, which have been recently extended to the use of several probes, such as Raman scattering,[21] electron diffraction,[22] angle-resolved photoemission,[23] and broadband optical spectroscopy.[24] All these techniques require an intense ultrashort pump laser pulse, ranging from 0.5 to several mJ/cm^2 (Refs. 23 and 22,

respectively), to obtain reliable results. Our results tackle the long-standing question of the effect of a pump laser pulse at high fluence on the superconducting condensate of HTSCs.

In Sec. II we briefly report the experimental procedure. In Sec. III A we study the temperature dependence of the signal related to the superconducting phase in the low-excitation regime and we show, within the context of the RT model,[25] that the decay rate is proportional to the superconducting order parameter Δ. In particular, we focus on the decay time divergence in the vicinity of T_c, where $\Delta \to 0$ and thus a vanishing relaxation rate is measured.[10,11,13,26]

In Sec. III B we discuss the dynamics as a function of fluence at a fixed temperature (10 K) well below T_c. Above a threshold pump fluence, the reflectivity variation deviates from the linear dependence and exhibits a saturation in agreement with previous experiments.[3,8,9] This discontinuity is identified with the condensate vaporization in the whole probed volume.[8] We observe the absence of a decay time divergence above this threshold, at variance with the quasithermal case (Sec. III A) and with experimental observations of PIPTs on CDW (Refs. 15,16) and SDW (Ref. 17) compounds.

To interpret the data in the high-fluence regime we take into account dynamical variations of the nonequilibrium superconducting gap, thus extending the RT model to the time-dependent case (Sec. III C). In Sec. III D we present the experimental data within the analytical results of the RT model. We obtain a linear decrease of the nonequilibrium gap with pump fluence and a finite nonequilibirum superconducting gap 2 ps after the pump pulse that causes the PIPT.

II. EXPERIMENTAL METHODS

Pump-probe measurements have been performed on an overdoped $Bi_2Sr_2Ca_{0.92}Y_{0.08}Cu_2O_{8+\delta}$ single crystal with $T_c = 78 \pm 5$ K. The Y-substituted Bi2212 single crystal was grown in an image furnace by the traveling-solvent floating-zone technique with a nonzero Y content in order to maximize T_c.[27] The crystal was annealed in flowing oxygen in order to increase the hole concentration and reach the overdoped side of the phase diagram. The sample was subsequently homogenized by further annealing in a sealed quartz ampoule, together with ceramic at the same oxygen content. In our experiments the 800 nm, 120 fs laser pulses are generated by a cavity-dumped Ti:sapphire oscillator. The use of a tunable repetition rate laser source allows us to avoid the experimental problem of average heating effects.[28] These effects prevented earlier observation of the photoinduced condensate vaporization.[6,7] In the time-resolved experiment the transient reflectivity variation is measured and we denote it as $\Delta R/R$.

III. RESULTS AND DISCUSSION

A. Low-fluence results as a function of temperature

In the low-intensity regime several common trends have been recognized based on the large amount of experimental data reported on HTSCs: (i) the appearence below T_c of a $\Delta R/R$ signal proportional to the photoexcited quasiparticle (QP) density,[3–14,26] (ii) an intensity- and temperature-dependent decay time of this superconducting component,[5,6,9–14,26] and (iii) the equivalence of the decay time

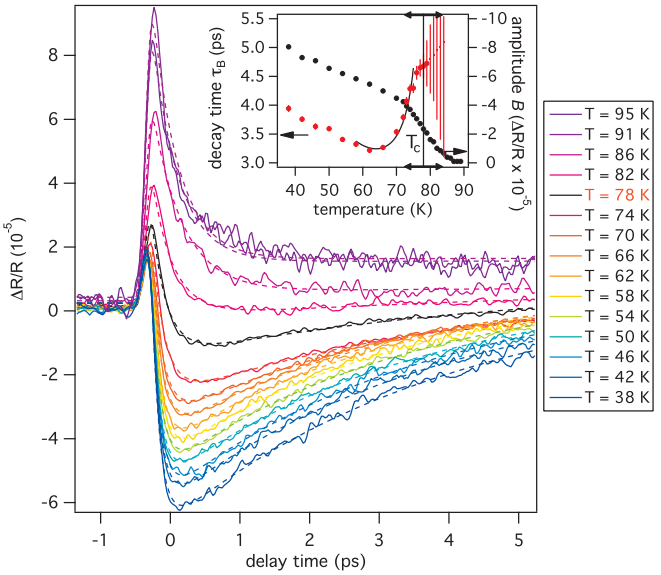

FIG. 1. (Color online) $\Delta R/R$ signal (solid lines) as a function of delay time at different temperatures (from 95 to 38 K) on a Y-Bi2212 overdoped single crystal. The dashed lines are the fits to the experimental curves (see the fitting function in the text). The black line represents the $\Delta R/R$ trace at T_c. In the inset we report the fit parameters of the SCS, i.e., decay time τ_B (red circles) and amplitude B (black circles). The error bars obtained from the fit procedure are displayed for all the data. The high uncertainty on the decay time above T_c led us to plot just the error bar and not the data point. The black arrow on the temperature axis of the inset shows the superconducting transition amplitude of the sample.

observed by probing at 800 nm and the gap dynamics observed in the terahertz spectral region.[14]

In Fig. 1 we plot the raw ($\Delta R/R$) data of consecutive series of scans taken from 95 down to 38 K at low pump fluence ($\sim 4\ \mu J/cm^2$). The positive signal above T_c can be reproduced by a single exponential decay function, Ae^{-t/τ_A}, convoluted with the time shape of the laser pulse, describing the relaxation of hot electrons via electron-phonon interaction[29–31] with a relaxation time τ_A of about 440 fs. All the traces from room temperature down to 95 K did not show any substantial difference from the 95 K trace. In agreement with the literature,[20] no $\Delta R/R$ sign change associated with the pseudogap phase is observed when probing at 800 nm wavelength on the overdoped sample, at variance with optimally and underdoped samples.[18]

The positive and fast signal survives also below T_c, superimposed on a negative signal that we recognize as the superconducting signal (SCS) proportional to the photoexcited QP density and that we capture with a single exponential function. The sum of these two functions, $Ae^{-t/\tau_A} + Be^{-t/\tau_B}$, is sufficient to reproduce all the experimental curves as shown in Fig. 1. The relevant fit parameters of the SCS, i.e., the amplitude B and the decay time τ_B, are plotted in the inset.

The decay time of the SCS, τ_B, is shown, as a function of temperature, in the inset of Fig. 1 (red circles). Starting from 38 K the decay time decreases with temperature, reaching a minimum at 62 K of 3.3 ps. Above this temperature it rapidly increases, reaching the value of 4.7 ps at T_c. At this temperature the order parameter vanishes ($\Delta \to 0$), the SCS amplitude

B is much smaller than A (the normal-state signal), and the uncertainty on the determination of its decay time strongly increases.

The increase in the decay time in the vicinity of T_c is in agreement with previous observations for other HTSCs in the low-fluence regime,[10,11,13,26] and it has been interpreted as the manifestation of a divergence proportional to $1/\Delta$ predicted by several theoretical calculations for BCS superconductors.[10,32,33] Experimentally, this divergence is smeared out because of the finite superconducting transition amplitude. However, from the analysis of the SCS decay time increase just below T_c, we can extract quantitative information about the superconducting gap.

A very useful model to interpret the nonequilibrium dynamics of superconductors in the low-intensity regime is the Rothwarf-Taylor model[13,25,34] (see the Appendix). In this model, two QPs recombine to form a Cooper pair emitting a boson with energy larger then 2Δ. As the reverse process is also allowed, the QP and the boson populations are in quasiequilibrium and the actual relaxation is determined by inelastic processes. Within this model, one can write down a set of coupled rate equations, which have analytic solutions in two very important limiting cases, the weak- and the strong-bottleneck regimes.[13,25] In the first case, the boson inelastic decay rate is fast and the relaxation dynamics is equivalent to simple bimolecular dynamics.[12,14] In the second regime, namely, the strong-bottleneck one, the inelastic decay of the boson population strongly slows down the relaxation process. For a given superconductor, the dynamical regime is determined by the particular type of bosons considered in this dynamics. However, in both regimes and far enough from the critical temperature,[35] a very simple formula for the QP decay rate γ is valid,

$$\gamma(T,\Delta(n_{\rm ph}),n_{\rm ph}) = (n_{\rm ph} + n_T)\Gamma(T,\Delta(n_{\rm ph})), \qquad (1)$$

where n_T are the thermal QPs, $n_{\rm ph}$ are the photoinjected ones, and $\Gamma(T,\Delta)$ is a function of the microscopic probabilities for the scattering events involving QPs and bosons.[13] Given the QP population densities $n_{\rm ph}$ and n_T, one can extract from the experimental QP decay rate γ the $\Gamma(T,\Delta)$ function in the low-excitation limit. We stress that the use of this formula does not imply any assumption on the particular boson involved in the nonequilibrium dynamics.

We use the well-known result obtained by Kabanov *et al.*[10] that, for a d-wave superconductor with a two-dimensional (2D) Fermi surface with nodes and for temperatures $k_BT \ll \Delta \sim 5k_BT_c$ (Ref. 37), the QP population at thermal equilibrium, n_T, has the form

$$n_T = 1.64N(0)(k_BT)^2/\Delta, \qquad (2)$$

where $N(0)$ is the density of states at the Fermi level and Δ is the gap value at equilibrium. The temperature dependence of n_T obtained from Eq. (2) is plotted in Fig. 2(a). To validate Eq. (2), we estimate n_T from the temperature dependence of the B amplitude (inset of Fig. 1) through the formula[13]

$$B(T) \propto \frac{2N_{\rm ph} + n_{\rm ph}}{\sqrt{1 + 16n_T^2 + 8n_T}}, \qquad (3)$$

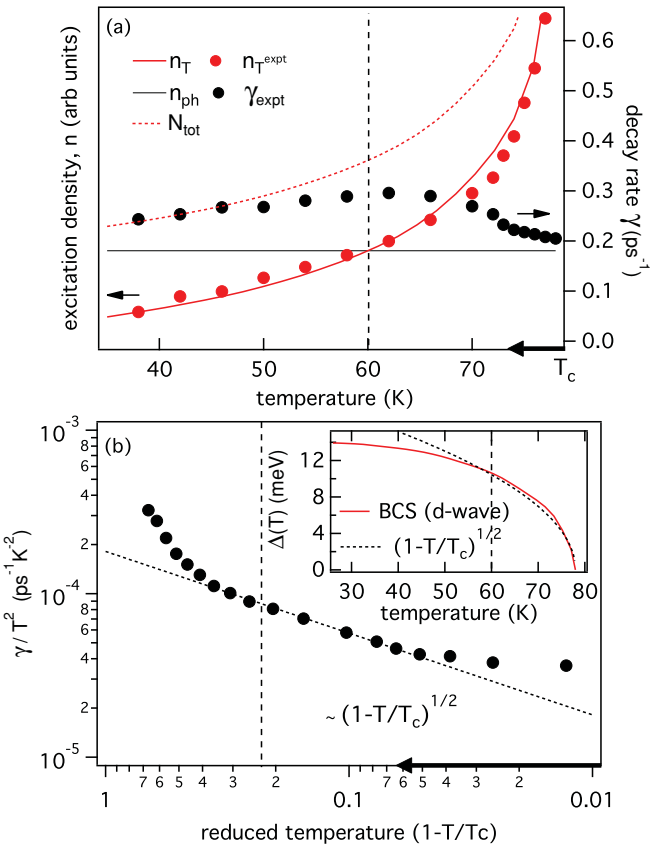

FIG. 2. (Color online) (a) Excitation density for both thermal and photoinduced QPs, respectively n_T and $n_{\rm ph}$ (solid lines), and their sum $N_{\rm tot}$ (dashed line) as a function of temperature. For the thermal QP we assumed Eq. (2) and a d-wave-like $\Delta(T)$ dependence and we compared the predicted value with the one obtained through Eq. (3) from the experimental $B(T)$ amplitude (inset of Fig. 1). On the right axis we report the experimental decay rate obtained from the fit in Fig. 1. (b) γ/T^2 as a function of the reduced temperature in a double-logarithmic plot. The long-dashed line represents the $(1 - T/T_c)^{1/2}$ power-law dependence. In the inset we show the result of the numerical integration of the d-wave BCS gap equation as a function of temperature compared to the $(1 - T/T_c)^{1/2}$ dependence (Ref. 36). In all the panels the vertical dashed lines divide the low- from the high-temperature regime (see text). In (b) the error bars are within the black circles' size.

where $N_{\rm ph}$ is the photoexcited boson population density and we assume, as in Refs. 13,26, the total population density $(n_{\rm ph} + 2N_{\rm ph})$ to be constant in temperature since the pump fluence is constant. The $B(T)$ amplitude in the low-temperature limit is measured at $T = 10$ K. Good agreement is found between n_T predicted by Eq. (2) and the value obtained from the experimental data through Eq. (3) [Fig. 2(a)]. Thus in the following we will use the value of n_T calculated through Eq. (2).

In Fig. 2(a) the experimental SCS decay rate γ and the total QP density $N_{\rm tot} = n_{\rm ph} + n_T$ are compared. The contribution due to $n_{\rm ph}$ is estimated in the low-temperature limit.[38]

In the high-temperature limit we observe that (i) the thermal population n_T is dominating over $n_{\rm ph}$; (ii) $\gamma_{\rm expt}$ is not following the $N_{\rm tot}$ temperature dependence. This finding suggests that the decay time increase observed close to T_c is related to a

decrease of $\Gamma(T,\Delta)$. We set the separation between the high- and low-temperature regimes at 60 K, i.e., when $n_T > n_{\rm ph}$. Our conclusions are independent of the particular choice of this temperature.

We now verify that the increase in decay time when approaching T_c is related to a real divergence arising from the fact that $\Gamma(T,\Delta) \to 0$ when $\Delta \to 0$ and we find the power-law that controls this divergence. In Fig. 2(b), we plot the quantity $\gamma_{\rm expt}/T^2$ as a function of the reduced temperature (distance from the critical temperature) on a double-logarithmic scale. Using Eqs. (1) and (2), we find that this quantity is proportional to

$$\frac{\gamma}{T^2} \propto \frac{\Gamma(T,\Delta)}{\Delta} \tag{4}$$

in the temperature region where n_T is the dominant term in the QP density, i.e., above 60 K.

In this region, we notice a power-law dependence,

$$\frac{\Gamma(T,\Delta)}{\Delta} \propto (1 - T/T_c)^{\tilde{\beta}} \tag{5}$$

with an exponent $\tilde{\beta} \sim 1/2$ [solid line in Fig. 2(b)], which is the same mean-field critical exponent expected for the order parameter Δ in a BCS superconductor. In a d-wave superconductor with T_c of 78 K, the superconducting gap dependence is well approximated by $\Delta \propto (1 - T/T_c)^{1/2}$, in the temperature range from 60 to 78 K [see the inset in Fig. 2(b)]. This assumption is still a good approximation in the case of overdoped HTSCs.[39–41] A deviation from this exponent is found a few degrees below T_c, since Eq. (1) is not applicable in the close vicinity of T_c.[35]

Within the approximate analytic solution [Eq. (1)],[35] we can easily derive the power-law dependence of the $\Gamma(T,\Delta)$ function in the RT approach:

$$\Gamma(T,\Delta) \propto (1 - T/T_c)^{\alpha} \propto \Delta^{2\alpha}, \tag{6}$$

where $\alpha \sim 1$ with an estimated uncertainty of about 30%. This power-law dependence can hardly be derived by first principles, particularly if the nature of the boson involved in the pairing mechanism is unknown.

B. Discontinuity in the fluence dependence

In Figs. 3(a) and 3(b), we report the $\Delta R/R$ traces at 10 K obtained at increasing pump intensity. Similarly to Sec. III A, all the curves were fitted using two exponential functions convoluted with the time shape of the laser pulse. The results of the fit are superimposed onto the experimental curves. Figure 3(c) shows the SCS amplitude and decay time for each fit as a function of pump fluence.

The low-excitation regime, i.e., the regime where the SCS is proportional to the pump fluence is reported in Fig. 3(a) and in Fig. 3(c) below 26 μJ/cm^2 $\equiv \Phi_C$. In agreement with previous works,[3–14,26] we assume that the SCS is proportional to the photoinduced QP density $n_{\rm ph}$. Thus we conclude that $n_{\rm ph}$ increases linearly with the pump fluence in this regime. In the zero-fluence limit, where $n_{\rm ph} \to 0$, we observe a divergence of the decay time [Fig. 3(c)]. This is related to Eq. (1), as the total QP density ($n_{\rm ph} + n_T$) becomes extremely small at low fluence and at low temperature (10 K).

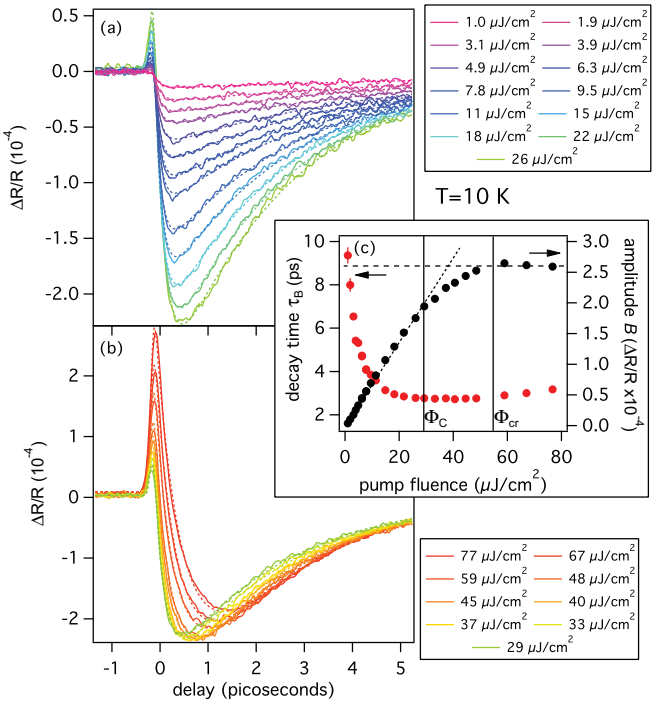

FIG. 3. (Color online) $\Delta R/R$ signal, solid lines in (a) and (b), at 10 K at different pump fluences. The fits to the experimental curves are shown with dashed lines. The fit parameters (decay time τ_B and amplitude B) are reported in (c) as a function of pump fluence. In (a) the low-intensity regime is shown, corresponding to $\Phi < \Phi_C$ in (c). The short-dashed line in (c) is the linear fit in the low-fluence regime. (b) and (c) for $\Phi > \Phi_C$ correspond to the high-excitation regime. The long-dashed line in (c) represents the saturation value. The error bars in (c) are within the circles' size.

Above Φ_C the SCS has a sublinear dependence and we identify this regime as the high-excitation regime[3,8] [Fig. 3(b) and Fig. 3(c) for $\Phi > \Phi_C$]. In this regime, the SCS exhibits a saturation at a critical fluence $\Phi_{\rm cr}$ of $\sim$55 μJ/cm^2. This saturation means that no more Cooper pairs can be destroyed above $\Phi_{\rm cr}$ and it is considered as evidence of the superconducting condensate vaporization during the laser pump pulse.[3,8] The fact that the crossover between the linear and the saturated regimes does not show an abrupt discontinuity here can be justified by the spatial profiles of the pump and probe light pulses.[8] The occurence of a real PIPT in this regime has been proved by measuring the emergence of a fast component above $\Phi_{\rm cr}$ in underdoped Bi2212 single crystals.[3] Similarly we observe in Fig. 3(b) an enhancement of the positive signal A associated with the fast e-ph free carrier relaxation.

We can compare the SCS in the case of the photoinduced [Fig. 3(c)] and the thermally induced phase transitions (inset of Fig. 1). In the former case, the parameter setting the level of perturbation of the system is the pump fluence, while in the latter case this role is played by the sample temperature. Within this analogy, the critical fluence $\Phi_{\rm cr}$, at which the SCS exhibits saturation, is the counterpart of the critical temperature T_c.

According to nonequilibrium superconductivity models,[1,2,42] a superconducting-to-normal-state PIPT can be either a first-order nonthermal phase transition[1,2] (μ^* model) or a quasithermal second-order phase transition (T^* model).[2,42]

In the T^* model the quasithermal condition is applied to electrons and high-frequency bosons, both being distributed with statistics at an effective temperature T^*. In both cases the saturation of the SCS reflects the impossibility of exceeding a critical QP density in the stable superconducting phase.[1–3,42]

In analogy to the thermal case (studied in Sec. III A), the quasithermal photoinduced vaporization would cause the superconducting order parameter to vanish at Φ_{cr}. Thus a diverging decay time should be measured, according to Eqs. (6) and (4), and in analogy to experimental results about the PIPTs in CDW (Refs. 15,16) and SDW (Ref. 17) compounds. On the contrary, the experimental results here reported show a decay time that remains finite and below 3.2 ps, thus excluding the quasithermal origin of the PIPT and suggesting a finite gap at the threshold fluence.

However, the connection between the decay time of the SCS and the superconducting gap is firmly established only in the low-fluence regime within the analytical results of the RT model[13] [Sec. III A, Eq. (6)]. To extend this concept to the high-fluence regime, when the nonequilibrium superconducting gap $\Delta(t)$ could strongly vary in time, a validation of the RT model is necessary.

Before we discuss this point in Sec. III C, we report two important experimental facts about the dynamics of the SCS (see Fig. 4):

(a) The relaxation dynamics is well reproduced by exponential decays (dashed lines) in the high-fluence regime, as in the low-fluence one. This decay is compatible with the RT model, where the gap is assumed to be constant in time, thus suggesting that the variations of $\Delta(t)$ are small.

(b) For $\Phi > \Phi_{cr}$, the decay dynamics collapse into a single curve, indicating that the nonequilibrium gap $\Delta(t)$ reaches its minimum value at Φ_{cr}, remaining the same at higher fluences.

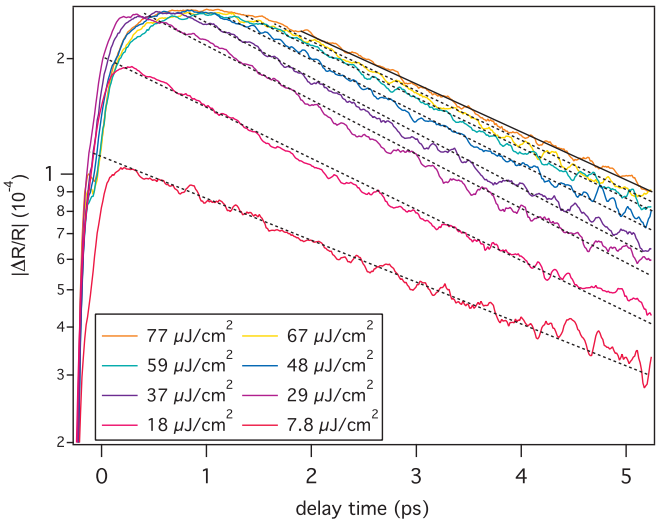

FIG. 4. (Color online) $|\Delta R/R|$ traces in logarithmic scale at several pump fluences at $T = 10$ K, where the exponential A component has been subtracted. The dashed lines represent the exponential fit of the decay. The solid line refers to the curve at $\Phi = 77\ \mu J/cm^2$.

C. Rothwarf-Taylor model in the high-fluence regime: A time-dependent approach

When a superconducting system is strongly perturbed through an ultrashort laser pulse, we expect the superconducting order parameter Δ to have strong variations in time. The parameters β, η, and γ_{esc} of the RT model (see the Appendix for definitions) are affected by these variations[10,43] and can vary in time. Therefore the high-perturbation limit requires a time-dependent Rothwarf-Taylor model. Herewith below we use the following assumptions:

(i) The time-dependent nonequilibrium superconducting gap $\Delta(n(t))$ can be expressed as a function of $n(t)$ by considering the T^* and μ^* models.[1,2,42] In both cases the normalized $\Delta(n(t))$ depends on $[1 - an(t)]$ [where $n(t)$ is the QP density and a a conversion factor] for an s-wave gap symmetry and $[1 - an(t)^{3/2}]$ for a d-wave gap symmetry.

(ii) $\beta(\Delta(n(t)))$ is constant, its temperature dependence being very weak, as reported on YBCO.[12]

(iii) $\eta(\Delta(n(t)))$ is determined with a fit of the rise time at low fluence (see the Appendix) and is set to a constant. This is a justified by the weak temperature dependence of the pair-breaking time[8,13] observed in pump-probe experiments at low fluence[12,18] (see Sec. III A).

(iv) $\gamma_{esc}(\Delta(n(t)))$ is the only time-dependent parameter and is responsible for the gap dependence of $\Gamma(T, \Delta)$, evidenced in Sec. III A [Eq. (6)]. The value corresponding to the unpertubed gap, $\gamma_{esc}(0)$, can be determined by a fit of the experimental decay at low fluence using the time-indepedent RT model. (See the Appendix.)

(v) Following a well-established trend in the literature[7,8,13,44] we assume that the cuprates are in the strong-bottleneck regime. We can thus conclude that $\Gamma \propto \gamma_{esc}$ (Ref. 13).

Under these approximations, the time-dependent RT equations are

$$\dot{n} = I_{QP}(t) + 2\eta p - \beta n^2, \tag{7}$$

$$\dot{p} = I_{ph}(t) - \eta p + \beta n^2/2 - \gamma_{esc}(t)(p - p_T), \tag{8}$$

with

$$\gamma_{esc}(t) = \gamma_{esc}(0)[\Delta(n(t))/\Delta(0)]^{2\alpha}, \tag{9}$$

where for an s-wave gap symmetry we have

$$\gamma_{esc}(t) = \gamma_{esc}(0)[1 - an(t)]^{2\alpha} \tag{10}$$

and for a d-wave gap symmetry

$$\gamma_{esc}(t) = \gamma_{esc}(0)[1 - an(t)^{3/2}]^{2\alpha} \tag{11}$$

with a being a conversion factor which set the perturbation of the nonequilibrium gap by QPs and α the exponent appearing in Eq. (6) determined in Sec. III A ($\alpha \sim 1$). The time-dependent RT equations [Eqs. (7) and (8)] are then integrated numerically and used to fit the experimental curves of the SCS.

In Fig. 5 we report the results relevant to a single experimental curve at $\Phi = \Phi_C$ and $T = 10$ K, where we assume a d-wave gap symmetry [Eq. (11)]. The determined a parameter is $(1.0 \pm 0.2) \times 10^{-20}$ cm^3. The agreement with the experimental data is very good. The predicted normalized nonequilibrium gap, $\Delta(t) \propto [\gamma_{esc}(t)]^{1/2\alpha}$, shows a minimum of 60% at the maximum SCS and an almost complete gap

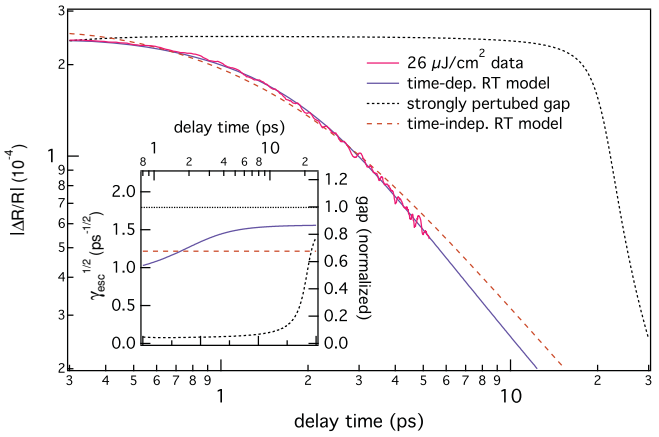

FIG. 5. (Color online) $|\Delta R/R|$ of the SCS at $\Phi = 26\ \mu\mathrm{J/cm}^2$ and the corresponding fit (solid line) obtained with the numerical solutions of the time-dependent Rothwarf-Taylor equations [Eqs. (7) and (8)] considering a d-wave gap symmetry. The a optimal value is $(1.0 \pm 0.2) \times 10^{-20}$ cm^3. For comparison we also show the fits when the parameter a is fixed to the values $a = 2.45 \times 10^{-20}$ cm^3 (short-dashed line) and $a = 0$ (long-dashed line), which is equivalent to the time-independent RT model. In the inset we show the corresponding function $[\gamma_{\mathrm{esc}}(t)]^{1/2}$, which is proportional to the nonequilibrium superconducting gap $\Delta(t)$ [Eq. (9)]. We normalized the gap to the low-fluence value.

relaxation (85%) after a time delay of 5 ps. Similar results are obtained considering an s-wave gap symmetry [Eq. (10)].

For comparison, we report also two fits where a is held constant with values $a = 0$, equivalent to the time-independent RT model, and $a = 2.45 \times 10^{-20}$ cm^3, where the gap is suppressed by $\approx$95%. In the latter case the predicted relaxation dynamics is extremely slow (of the order of several tens of picoseconds) and strongly nonexponential. Both these characteristics are incompatible with the experimental curve reported in Fig. 5, thus indicating that, below Φ_C, the nonequilibrium gap is never close to zero.

Above Φ_C, the universal and exponential decay dynamics mentioned in Sec. III B suggests a finite nonzero gap after 1–2 ps. It is possible to estimate a lower bound for this finite nonequilibrium gap, considering the optimal a parameter and extracting $\Delta(n(t))_{\mathrm{min}}$ from the maximum SCS for each curve in Fig. 4. The result is that, at any time instant t where the RT model is applicable, the condition $\Delta(t) > \frac{1}{2}\Delta(0)$ is realized.

D. Scenarios for a superconducting-to-normal dynamical phase transition

Although the time-dependent RT model discussed in the previous section provides a remarkably good description of the experimental data, we observe that the time-independent RT model is also a valid approximation, provided an average gap value (corresponding to the value predicted by the time-dependent approach at ~2 ps delay) is assumed. In particular we demonstrated that in our experimental conditions we have $\Delta(n_{\mathrm{ph}}, 10\ \mathrm{K}) > \frac{1}{2}\Delta(0, 10\ \mathrm{K})$; thus we can estimate the maximum density of photoexcited QPs, $n_{\mathrm{ph}} < n_{T=70\ \mathrm{K}} \ll \eta/\beta$ [according to the inset of Fig. 2(b) and Ref. 2]. This condition ensures the validity of the analytical formulas obtained in Sec. III A.

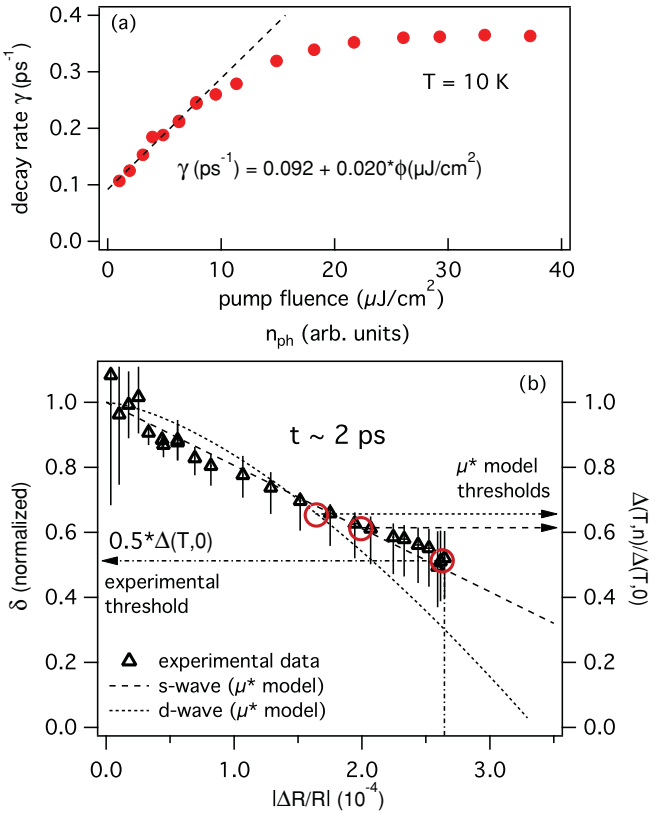

FIG. 6. (Color online) (a) Experimental decay rate extracted by the fit of the $|\Delta R/R|$ traces at different pump fluences (see Fig. 3). The dashed line is the linear fit obtained in the low-intensity limit. The error bars are within the circles' size. (b) δ as a function of $|\Delta R/R|$. We normalized the value to the zero-fluence limit, which correspond to the equilibrium gap $\Delta(T,0)$. The error bars account both for the 30% uncertainty in the determination of α and for the difference between the results obtained within the analytic and the numerical solutions of the RT equations (see text). On the same graph (right and upper axes) we show the analytical results of the μ^* model for the superconducting gap Δ as a function of QP density n_{ph} as reported in Ref. 2 for both s-wave and d-wave cases. The threshold values are calculated numerically within the μ^* model (Ref. 2) at a finite temperature corresponding to 10 K in our experiment.

We recall Eq. (1) and, plotting the decay rate as a function of pump fluence [Fig. 6(a)], we observe the expected linear dependence at low fluence. The intercept of 0.092 ps^{-1} is related to the finite value of n_T at $T = 10$ K. This linear dependence on the pump fluence follows the trend observed on underdoped HTSCs, [6,12] but was not observed clearly on overdoped samples. [6,45] We define an effective photoinduced decay rate γ_{ph},

$$\gamma_{\mathrm{ph}}(T, \Delta(n_{\mathrm{ph}}), n_{\mathrm{ph}}) \equiv \gamma(T, \Delta(n_{\mathrm{ph}}), n_{\mathrm{ph}}) - \gamma_T(T, \Delta(0), n_{\mathrm{ph}} = 0), \qquad (12)$$

that represents the decay rate exclusively due to the photoinjected QPs, where the thermal contribution to the decay rate, γ_T, [intercept in Fig. 6(a)] has been subtracted. We neglect the sample temperature dependence since in our pump-probe

experiment this parameter remains constant. We thus obtain the formula

$$\begin{aligned}\gamma_{\rm ph}(\Delta(n_{\rm ph}),n_{\rm ph}) &= n_{\rm ph}\Gamma(\Delta(n_{\rm ph})) + n_T[\Gamma(\Delta(n_{\rm ph})) - \Gamma(\Delta(0))] \\ &\approx n_{\rm ph}\Gamma(\Delta(n_{\rm ph})). \end{aligned} \quad (13)$$

In the right-hand side of Eq. (13) we neglected the second term of the sum. This approximation is valid in the high-excitation regime when $n_{\rm ph}$ is much larger than n_T, as long as Γ is not going to zero, which is suggested by the absence of a decay time divergence.

Using Eq. (6) and the proportionality between $n_{\rm ph}$ and $\Delta R/R$ we can rewrite Eq. (13) as

$$\gamma_{\rm ph} = \frac{\Delta R}{R}\Delta^{2\alpha}, \quad (14)$$

from which we obtain

$$\left(\frac{\gamma_{\rm ph}}{\Delta R/R}\right)^{1/2\alpha} \propto \Delta. \quad (15)$$

We thus define the quantity $\delta \equiv (\frac{\gamma_{\rm ph}}{\Delta R/R})^{1/2\alpha}$, proportional to the nonequilibrium superconducting gap Δ, and we assume $\alpha \sim 1$ (Sec. III A).

In Fig. 6(b) we report the value of this quantity, normalized to the zero-fluence-limit value, obtained from the experimental curves of Fig. 3 as a function of the SCS amplitude. The gap value decreases with $\Delta R/R$; hence it decreases with increasing $n_{\rm ph}$, as expected.[1,2,42] On the other side, above the experimental threshold, where $n_{\rm ph}$ is constant, the nonequilibrium gap remains constant, reflecting the correctness of neglecting the T dependence in $\Delta(n_{\rm ph},T)$ and $\gamma_{\rm ph}(T,\Delta,n_{\rm ph})$.

The experimental data are here compared to the predictions of the μ^* model, where a first-order phase transition is expected.[1–3] Within this model the nonequilibrium QP population is described by a Fermi-Dirac distribution with an effective chemical potential μ^*, while its temperature remains at the equilibrium value T. In Fig. 6(b) we plot the analytical results for $\Delta(n,T=0)/\Delta(n=0,T=0)$ in the low-excitation limit as a function of the QP density n for both s-wave and d-wave gap symmetries.[2] The dependence in the d-wave case is proportional to $n^{3/2}$, while it is linear in the s-wave case, as reported in the previous section.

The μ^* model predicts a superconducting-to-normal-state phase transition at a finite gap value, when the superconducting-state free energy increases above the normal-state value. At 10 K this phase transition should take place at relative gap values of ≈60% and ≈65% in the s-wave and d-wave cases, respectively[2] [Fig. 6(b)].

The main features evidenced by the experimental data reported in Fig. 6 are (i) a finite value of $\Delta(n_{\rm max},T=10\ {\rm K})$ of about 1/2 of the equilibrium value at the fluence threshold $\Phi_{\rm cr}$, and (ii) the linear dependence of $\Delta(n_{\rm ph},T=10\ {\rm K})$ with $\Delta R/R$ and thus with $n_{\rm ph}$.

The result (i) self-consistently confirms our initial assumption of a nonvanishing Γ function and of $\Delta(n_{\rm ph},10\ {\rm K}) > \frac{1}{2}\Delta(0,10\ {\rm K})$. The experimental value obtained in this work is remarkably close to the μ^* model predictions, even though a quantitative comparison would require a detailed analysis of the photoinduced QP distribution in the k-space and accurate numerical calculations in the high-fluence regime.[2,3]

The result (ii) suggests an s-wave-like dependence of the nonequilibrium gap. Even though this finding seems in contradiction with the equilibrium gap d-wave symmetry reported for HTSCs,[46] one should bear in mind that the nonequilibrium population photoinduced by a 100 fs laser pulse in a d-wave superconductor is mostly peaked in the antinodal region[47] because of energy-momentum conservation constraints.[12,48] This leads to a nonthermal effective distribution that can be reproduced by Fermi-Dirac statistics with anisotropic effective chemical potential.

The results of such an anisotropic model are equivalent to those obtained for an s-wave superconductor. An s-wave-like gap symmetry was previously used to explain the temperature dependence of $n_{\rm ph}$ in the low-excitation regime of HTSCs,[10] and led to a strong controversy in the interpretation of pump-probe experiments.[2,10] We remark that this result does not imply an s-wave gap symmetry in HTSCs at equilibrium and is rather related to the excitation process.

Both these results suggest a strongly nonthermal QP population distribution, thus opening two possible physical scenarios behind the superconducting-to-normal PIPT: (i) the first-order dynamical phase transition predicted by the μ^* model[1–3] and supported by the time-dependent RT model (Sec. III C); (ii) a second-order transition with a quick (<1–2 ps) gap recovery, where the fundamental assumptions of the RT model break down on the short time scales in the high-excitation regime.

The second scenario goes beyond the treatment proposed in Sec. III C as the phonon bottleneck would be avoided on short time scales due to the highly nonthermal QP distribution. The breakdown of the RT equations implies the decoupling of the relaxation dynamics of QPs and high-frequency bosons, suggesting the nonthermal character of the PIPT, in contrast with the quasithermal PIPT predicted by the T^* model.[2,42] Within the first picosecond the superconducting state is recovered with a finite nonequilibrium gap, as demonstrated in this section.

However the time-dependent RT model reproduces very precisely the experimental dynamics at Φ_C (Fig. 5, Sec. III C), thus suggesting the validity of this model at excitation levels quite close to the PIPT. Thus, while the nonthermal second-order phase transition implies an abrupt breakdown of this model between Φ_C and $\Phi_{\rm cr}$, the nonthermal first-order transition is compatible with the time-dependent RT model also above $\Phi_{\rm cr}$.

The results reported in this paper are obtained assuming the validity of Eq. (1), which is an approximated analytic solution of the time-independent RT equations.[35] We repeated the same procedure starting from the numerical solution of the time-indepedent RT equations, which is valid in the whole temperature and fluence range. However, the final results of our work are unaffected. The error bars in Fig. 6(b) account for the deviation of the analytic results from the numerical ones and for a 30% uncertainty in the determination of α.

Both the hypotheses proposed in this section have a nonthermal character, at variance with the quasithermal PIPT reported on other systems, such as CDW (Refs. 15,16) and SDW (Ref. 17) systems. Since the photoexcitation process is

the same, this remarkable difference calls for a deeper understanding of the nonequilibrium QP and boson thermalization processes in HTSCs compared to CDW and SDW compounds.

IV. CONCLUSION

We reported pump-probe experiments on an overdoped Y-Bi2212 sample at 800 nm. We explored both the low- and the high-excitation regimes to study the origin of the recently discovered photoinduced vaporization of the superconducting condensate.[3,8] We first verified the exponent of the power-law divergence at low excitation in the vicinity of T_c.

In the high-excitation regime, we showed a lack of the quasiparticle decay time increase at the fluence required to photoinduce the transition, in contrast to previously reported PIPTs on CDW (Refs. 15,16) and SDW (Ref. 17) systems. At that fluence ($\Phi_{cr} \approx 55\ \mu J/cm^2$) we estimated a finite nonequilibrium gap value (2 ps after the interaction with the pump pulse) of about 1/2 of the equilibrium gap.

This finding proves the nonthermal character of the superconducting-to-normal-state PIPT, leading to two possible phase transition mechanisms: (i) a first-order dynamical phase transition predicted by the μ^* nonequilibrium superconductivity model,[1–3] and supported by numerical solutions of an extended time-dependent RT model, and (ii) a second-order transition with a quick gap recovery, where the fundamental assumptions of the RT model abruptly break down in the high-excitation regime on short time scales (t < 1–2 ps).

These findings tackle the fundamental question about the interaction of an infrared coherent pulse with the superconducting condensate in HTSCs at high excitation pump intensity. This is a landmark for the growing field of pump-probe techniques on HTSCs.[3,8,9,21–24,26,49] Our experiment defines the maximum pump fluence ($\Phi_{cr} \approx 55\ \mu J/cm^2$) which still allows one to probe the superconducting state of overdoped Y-Bi2212; it also demostrates that recent pump-probe experiments perfomed on Bi2212 at higher pump fluences[21–23] are dealing with a dynamical competing admixture of superconducting, normal, and possibly pseudogap phases.

The considerable difference between the PIPTs in HTSCs and those in CDW (Refs. 15 and 16) and SDW (Ref. 17) systems suggests a need for a deeper understanding of the fundamental distinctions in the nonequilibrium properties of these compounds.

ACKNOWLEDGMENTS

F.C., G.C., and F.P. acknowledge the support of the Italian Ministry of University and Research under Grants No. FIRBRBAP045JF2 and No. FIRB-RBAP06AWK3. The crystal growth work was supported by DOE under Contracts No. DE-FG03-99ER45773 and No. DE-AC03-76SF00515 and by NSF under Grant No. DMR9985067.The work at UBC was supported by the Killam Program (A.D.), the Alfred P. Sloan Foundation (A.D.), the CRC Program (A.D.), NSERC, CFI, CIFAR Quantum Materials, and BCSI.

APPENDIX: ROTHWARF-TAYLOR EQUATIONS

The nonequilibrium dynamics in superconductors is usually successfully interpreted[12,13] within the phenomenological frame of the Rothwarf-Taylor equations,[25]

$$\dot{n} = I_{QP}(t) + 2\eta p - \beta n^2, \tag{A1}$$

$$\dot{p} = I_{\rm ph}(t) - \eta p + \beta n^2/2 - \gamma_{\rm esc}(p - p_T), \tag{A2}$$

describing the density of excitations n coupled to phonons, p being the gap-energy phonon density. The nonequilibrium QPs and phonons are photoinjected into the system through the $I_{QP}(t)$ and $I_{\rm ph}(t)$ terms. A Gaussian temporal profile of $I_{QP}(t)$ and $I_{\rm ph}(t)$, with the same time width as the laser pulse, is assumed. The coupling of the electronic and phonon populations is obtained through (a) the annihilation of a Cooper pair via gap phonon absorption ($p\eta$ term) and (b) the emission of gap phonons during the two-body direct recombination of excitations to form a Cooper pair (βn^2 term). In the phonon bottleneck regime ($\eta > \gamma_{\rm esc}$) the excitation relaxation is ultimately regulated by the escape rate of the nonequilibrium gap-energy phonons [$\gamma_{\rm esc}(p - p_T)$ term, p_T being the thermal phonon density]. The $\gamma_{\rm esc}$ value is determined both by the escape rate of the nonequilibrium phonons from the probed region and by the energy relaxation through inelastic scattering with the thermal phonons. The $\Delta R/R$ superconducting signal is assumed to be proportional to the solution $n(t)$ of Eq. (A1), in agreement with previous works.[3–14,26] At low fluence ($\Phi < \Phi_C$), the SCS reported in Fig. 4 is satisfactorily reproduced by considering only the $I_{\rm ph}(t)$ term, i.e., assuming that the pump energy is mainly absorbed through excitation of the phonon population. This result is in agreement with both theoretical predictions within the T^* model[2] and experimental observations on YBCO (Refs. 50,51) and MgB_2.[34] In the fitting procedure we assume $\beta = 0.1\ cm^2/s$, as reported in the literature.[12] The determined free parameters at low fluence ($\Phi = 1\ \mu J/cm^2$) are $\gamma = (4.5 \pm 0.5)\ ps^{-1}$ and $\gamma_{\rm esc} = (3.3 \pm 0.1)\ ps^{-1}$. These values are compatible with both the results obtained on $La_{2-x}Sr_xCuO_4$,[8] and the theoretical estimations of anharmonic processes in YBCO.[10]

[1] C. Owen and D. Scalapino, Phys. Rev. Lett. **28**, 1559 (1972).
[2] E. J. Nicol and J. Carbotte, Phys. Rev. B **67**, 214506 (2003).
[3] C. Giannetti, G. Coslovich, F. Cilento, G. Ferrini, H. Eisaki, N. Kaneko, M. Greven, and F. Parmigiani, Phys. Rev. B **79**, 224502 (2009).
[4] P. Gay, D. Smith, C. Stevens, C. Chen, G. Yang, S. Abell, D. Wang, J. Wang, Z. Ren, and J. Ryan, J. Low Temp. Phys. **117**, 1025 (1999).
[5] P. Gay, C. Stevens, D. Smith, C. Chen, and J. Ryan, Physica C **341**, 2221 (2000).
[6] N. Gedik, M. Langner, J. Orenstein, S. Ono, Y. Abe, and Y. Ando, Phys. Rev. Lett. **95**, 117005 (2005).

[7] G. Coslovich *et al.*, in *Lectures on the Physics of Strongly Correlated Systems XIII*, edited by A. Avella and F. Mancini, AIP Conf. Proc. No. 1162 (AIP, Melville, NY, 2009), p. 177.
[8] P. Kusar, V. V. Kabanov, S. Sugai, J. Demsar, T. Mertelj, and D. Mihailovic, Phys. Rev. Lett. **101**, 227001 (2008).
[9] T. Mertelj, V. V. Kabanov, C. Gadermaier, N. Zhigadlo, S. Katrych, J. Karpinski, and D. Mihailovic, Phys. Rev. Lett. **102**, 117002 (2009).
[10] V. V. Kabanov, J. Demsar, B. Podobnik, and D. Mihailovic, Phys. Rev. B **59**, 1497 (1999).
[11] D. Dvorsek, V. Kabanov, J. Demsar, S. Kazakov, J. Karpinski, and D. Mihailovic, Phys. Rev. B **66**, 020510 (2002).
[12] N. Gedik, P. Blake, R. Spitzer, J. Orenstein, R. Liang, D. Bonn, and W. Hardy, Phys. Rev. B **70**, 014504 (2004).
[13] V. V. Kabanov, J. Demsar, and D. Mihailovic, Phys. Rev. Lett. **95**, 147002 (2005).
[14] R. A. Kaindl, M. A. Carnahan, D. S. Chemla, S. Oh, and J. N. Eckstein, Phys. Rev. B **72**, 060510 (2005).
[15] A. Tomeljak, H. Schäfer, D. Städter, M. Beyer, K. Biljakovic, and J. Demsar, Phys. Rev. Lett. **102**, 066404 (2009).
[16] R. Yusupov, T. Mertelj, V. V. Kabanov, S. Brazovskii, P. Kusar, J.-H. Chu, I. R. Fisher, and D. Mihailovic, Nature Phys. **6**, 681 (2010).
[17] S. Watanabe, R. Kondo, S. Kagoshima, and R. Shimano, Phys. Rev. B **80**, 220408 (2009).
[18] Y. H. Liu, Y. Toda, K. Shimatake, N. Momono, M. Oda, and M. Ido, Phys. Rev. Lett. **101**, 137003 (2008).
[19] P. A. Lee, N. Nagaosa, and X. Wen, Rev. Mod. Phys. **78**, 17 (2006), and references therein.
[20] J. Demsar, B. Podobnik, V. V. Kabanov, T. Wolf, and D. Mihailovic, Phys. Rev. Lett. **82**, 4918 (1999).
[21] R. Saichu, I. Mahns, A. Goos, S. Binder, P. May, S. Singer, B. Schulz, A. Rusydi, J. Unterhinninghofen, D. Manske *et al.*, Phys. Rev. Lett. **102**, 177004 (2009).
[22] F. Carbone, D. Yanga, E. Giannini, and A. H. Zewail, Proc. Natl. Acad. Sci. USA **105**, 20161 (2008).
[23] L. Perfetti, P. A. Loukakos, M. Lisowski, U. Bovensiepen, H. Eisaki, and M. Wolf, Phys. Rev. Lett. **99**, 197001 (2007).
[24] C. Giannetti, G. Zgrablic, C. Consani, A. Crepaldi, D. Nardi, G. Ferrini, G. Dhalenne, A. Revcolevschi, and F. Parmigiani, Phys. Rev. B **80**, 235129 (2009).
[25] A. Rothwarf and B. Taylor, Phys. Rev. Lett. **19**, 27 (1967).
[26] E. E. M. Chia, D. Talbayev, J.-X. Zhu, H. Q. Yuan, T. Park, J. D. Thompson, C. Panagopoulos, G. F. Chen, J. L. Luo, N. L. Wang *et al.*, Phys. Rev. Lett. **104**, 027003 (2010).
[27] H. Eisaki, N. Kaneko, D. L. Feng, A. Damascelli, P. K. Mang, K. M. Shen, Z. X. Shen, and M. Greven, Phys. Rev. B **69**, 064512 (2004).
[28] High-pump-fluence measurements were performed at a repetition rate of 108 kHz or less, while low-pump-fluence ones were obtained at a repetition rate of 540 kHz to maximize the signal-to-noise ratio. The total photon intensity impinging the sample was never higher than 350 μW.
[29] P. B. Allen, Phys. Rev. Lett. **59**, 1460 (1987).
[30] S. D.Brorson, A. Kazeroonian, J. S. Moodera, D. W. Face, T. K. Cheng, E. P. Ippen, M. S. Dresselhaus, and G. Dresselhaus, Phys. Rev. Lett. **64**, 2172 (1990).
[31] S. Brorson *et al.*, Solid State Commun. **74**, 1305 (1990).
[32] M. Tinkham and J. Clarke, Phys. Rev. Lett. **28**, 1366 (1972).
[33] A. Schmidt and G. Schon, J. Low Temp. Phys. **20**, 207 (1975).
[34] J. Demsar, R. D. Averitt, A. J. Taylor, V. V. Kabanov, W. N. Kang, H. J. Kim, E. M. Choi, and S. I. Lee, Phys. Rev. Lett. **91**, 267002 (2006).
[35] Equation (1) is valid as long as $n_T \ll N_T$, where N_T is the boson population density at equilibrium. The limit $n_T \sim N_T$ is achieved only in the close vicinity of T_c (see Ref. [13]). Figure 2(a) clearly shows that n_T decreases rapidly below T_c, setting the condition $n_T \ll N_T$. Thus we assume Eq. (1) to be valid a few degrees below T_c.
[36] M. Tinkham, *Introduction to Superconductivity* (McGraw-Hill, New York, 1996).
[37] S. Hufner, M. A. Hossain, A. Damascelli, and G. A. Sawatzky, Rep. Prog. Phys. **71**, 062501 (2008).
[38] To obtain the value of the constant $n_{\rm ph}$ contribution to the decay rate we use the experimental values of γ at 38 K [Fig. 2(a)] and at 10 K, ~ 4 μJ/cm^2 [Fig. 6(a)]. We assume $\Gamma(T,\Delta)$ to be constant below 40 K [inset of Fig. 2(b)] and $n_T(10\ {\rm K}) = 0$. Thus we have $\gamma(38\ {\rm K}) = \Gamma_0(n_T + n_{\rm ph})$ and $\gamma(10\ {\rm K}) \sim \Gamma_0(n_{\rm ph})$, from which we derive both Γ_0 and $n_{\rm ph}$.
[39] W. S. Lee, I. M. Vishik, K. Tanaka, D. H. Lu, T. Sasagawa, N. Nagaosa, T. P. Devereaux, Z. Hussain, and Z. Shen, Nature (London) **450**, 81 (2007).
[40] S. Hufner and F. Muller, Phys. Rev. B **78**, 014521 (2008).
[41] A. Yazdani, J. Phys. Condens. Matter **21**, 164214 (2009).
[42] W. Parker, Phys. Rev. B **12**, 3667 (1975).
[43] J. Unterhinninghofen, D. Manske, and A. Knorr, Phys. Rev. B **77**, 180509 (2008).
[44] N. Cao, Y. Wei, J. Zhao, S. Zhao, Q. Yang, Z. Zhang, and P. Fu, Chin. Phys. Lett. **25**, 2257 (2008).
[45] The slope obtained in this work in the range from 1 to 10 μJ/cm^2 is 0.02 ps^{-1}/μJ/cm^2, which is compatible, within the experimental uncertainty, with the substantially constant decay rate measured by Gedik *et al.*[6] in the range from 0.1 to 1 μJ/cm^2.
[46] W. N. Hardy, D. A. Bonn, D. C. Morgan, R. Liang, and K. Zhang, Phys. Rev. Lett. **70**, 3999 (1993).
[47] R. Cortes, L. Rettig, Y. Yoshida, H. Eisaki, M. Wolf, and U. Bovensiepen, e-print arXiv:1011.1171.
[48] P. C. Howell, A. Rosch, and P. J. Hirschfeld, Phys. Rev. Lett. **92**, 037003 (2004).
[49] F. Cilento *et al.*, Appl. Phys. Lett. **96**, 021102 (2010).
[50] S. G. Han, Z. V. Vardeny, K. S. Wong, O. G. Symko, and G. Koren, Phys. Rev. Lett. **65**, 2708 (1990).
[51] A. Frenkel, Phys. Rev. B **48**, 9717 (1993).